Hydrodynamic Shaping, Polymerization, and Subsequent Modification of Thiol Click Fibers

ARTICLE *in* ACS APPLIED MATERIALS & INTERFACES · DECEMBER 2012

Impact Factor: 6.72 · DOI: 10.1021/am3022834 · Source: PubMed

4 AUTHORS, INCLUDING:

Darryl Boyd
United States Naval Research Laboratory
15 PUBLICATIONS **94** CITATIONS
SEE PROFILE

Adam Shields
18 PUBLICATIONS **480** CITATIONS
SEE PROFILE

Jawad Naciri
United States Naval Research Laboratory
129 PUBLICATIONS **2,546** CITATIONS
SEE PROFILE

ACS APPLIED MATERIALS & INTERFACES

Research Article

www.acsami.org

Hydrodynamic Shaping, Polymerization, and Subsequent Modification of Thiol Click Fibers

Darryl A. Boyd,[‡] Adam R. Shields,[‡] Jawad Naciri, and Frances S. Ligler*

Center for Bio/Molecular Science & Engineering, Naval Research Laboratory, 4555 Overlook Avenue SW, Washington, D.C. 20375, United States

Supporting Information

ABSTRACT: Hydrodynamic focusing in microfluidic channels is used to produce highly uniform, shaped polymer fibers at room temperature and under "green" conditions. Core streams of thiol−ene and thiol−yne prepolymer solutions were guided using a phase-matched sheath stream through microfluidic channels with grooved walls to determine shape. Size was dictated by the ratio of the flow rates of the core and sheath streams. Thiol click reactions were initiated using UV illumination to lock in predesigned cross-sectional shapes and sizes. This approach proved to be much more flexible than electrospinning in that highly uniform fibers can be produced from prepolymer solutions with varying compositions and viscosities with made-to-order sizes and shapes. Furthermore, a very simple manipulation of the composition provided reactive groups on the fiber surface for attachment of active ligands and biological components. A proof-of-principle experiment demonstrated that biotin attached to thiol groups on the fiber surface could specifically bind a fluorescent protein.

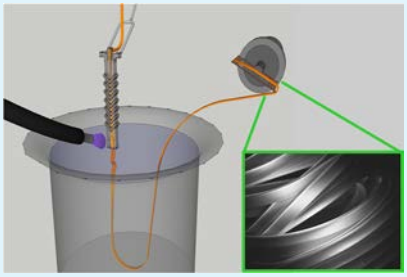

KEYWORDS: *click chemistry, hydrodynamic focusing, microfibers, microfluidics, thiol−ene, thiol−yne*

INTRODUCTION

Thiol click chemistry, a subset of the well-known click chemistry family of reactions, is emerging as a prominent synthetic method. Though some of the reactions included in this category were reported several decades ago,[1−3] thiol click reactions have resurfaced in the years since the versatility of click reactions has become evident.[4−6] The utility of materials made using thiol click chemistry is exemplified in applications as diverse as hydrogel drug delivery,[7−10] dendrimer synthesis,[11,12] high strength laminates,[13] dental resins,[14,15] and electroluminescent films.[16]

A primary advantage of thiol click materials is that simple changes in prepolymer composition can give rise to significant alterations in polymer properties. For example, slight variations in alkyl chain length can notably alter the water contact angle of films made via thiol click reactions.[17] In addition, prepolymer stoichiometric ratios can be adjusted to provide an excess of alkene/alkyne or thiol groups that remain unreacted following polymerization, thus rendering the polymerized material functionally active for subsequent modification. The growing body of work on thiol click materials is largely based on thin films and bulk materials, in part for the obvious reason that they are easy to produce. However, the advantages of fibers for use in polymer materials are well-known and include enhanced surface area-to-volume and strength-to-weight ratios, the permeability of fiber mats, and the ability to be woven into textiles.

One recent report has described a method for fabricating thiol click fibers. This 2011 report utilized electrospinning to synthesize fibers formed via thiol−ene click chemistry, with an emphasis on the solvent-free, and thus "green," nature of the reaction.[18] However, in order to electrospin well-formed fibers, the material composition was tightly constrained to a 1:4.4 ratio of thiol−alkene. This constraint was due to the interplay of factors such as viscosity versus surface tension and ultraviolet (UV) light exposure time versus curing kinetics, which are inherent issues with electrospinning. In addition, the constraint on solution viscosity also limited the method to the production of fibers at a single diameter of ∼25 μm. Slight deviations from the 1:4.4 thiol−ene ratio generated insufficiently cured fibers (1:5.6 ratio) and fibers with droplet defects (1:3.4 ratio). Herein we demonstrate fabrication of thiol click fibers via hydrodynamic focusing and UV exposure in a microfluidic channel. As opposed to the previous report, our method is significantly less constrained with regards to the prepolymer composition and does not suffer from the need to tightly control as many experimental and environmental parameters as with electrospinning. Using this method, we demonstrate (1) control over fiber size and cross-sectional shape, (2) the ability to employ various thiol click chemistries, (3) adaptability for prepolymer solutions of differing viscosities, leading to fabrication of thiol−yne fibers as well as thiol−ene fibers, and (4) the capacity to produce fibers with reactive groups available for subsequent surface modification. Thus, this straightforward method is well-suited for exploiting the advantages of thiol click chemistry to fabricate fibers. The work presented covers several research areas of interest including polymer chemistry (photopolymerization and click reactions) and polymer engineering

Received: October 10, 2012
Accepted: December 6, 2012
Published: December 6, 2012

(microfluidic fabrication and shaping of microfibers) as well as surface chemistry and biological modification (attachment of a fluorescent probe via protein linkage).

RESULTS AND DISCUSSION

Thiol Click Chemistry. The thiol click reactions presented in this work occur by the covalent attachment of an available sulfhydryl group to an alkene or an alkyne via a radical-mediated step growth polymerization.[6,19,20] The process can be expedited by ultraviolet light exposure,[21] including reactions proceeding in the mere presence of sunlight.[22]

To highlight the versatility of this fabrication process, we generated fibers using various thiol click solution compositions with a wide range of viscosities. The components chosen as the focus for this study were pentaerythritol tetrakis (3-mercaptopropionate) (PETMP), 1,7-octadiyne (ODY), and 1,4-butanediol divinyl ether (BDDVE), the structures of which are shown in Chart 1. PETMP is a tetrathiol that reacts with the

Chart 1. Components Used in Fabricating Thiol−yne (PETMP + ODY) and Thiol−ene (PETMP + BDDVE) Fibers

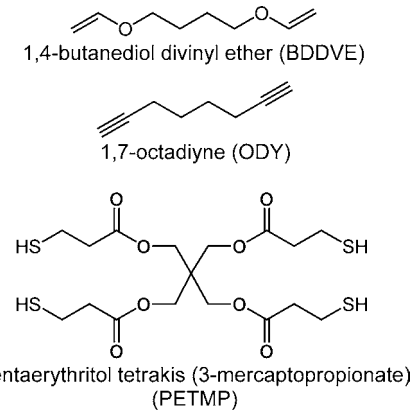

π bonds of ODY and BDDVE via a photoinitiation reaction. The addition of the photoinitiator 2,2-dimethoxy-2-phenyl-acetophenone (DMPA) to the reaction solution dramatically increased the rate of the reaction.[23,24] Since ODY has two π bonds for each of its terminal alkyne groups, PETMP reacts with ODY in a 1:1 ratio to form thiol−yne. Because BDDVE has only one π bond per vinyl group, two BDDVE react with one PETMP to form thiol−ene. At room temperature, the viscosity of the thiol−yne solution was ~60 cP, whereas the thiol−ene viscosity was ~30 cP.

Other components used to demonstrate the versatility of this fiber fabrication method included the dithiol 1,6-hexanedithiol (HxDT), the trialkene (1,3,5-triallyl-1,3,5-triazine-2,4,6 (1*H*,3*H*,5*H*)-trione (TATATO), and the dialkyne 1,6-heptadiyne (HpDY). The structures for each of these compounds, as well as a table of the specific combinations used, are found in the Supporting Information.

Fiber Fabrication. The fiber fabrication system utilizes hydrodynamic focusing in order to generate laminar flow in which a prepolymer (the core fluid) is ensheathed by a nonpolymerizable fluid (the sheath fluid) of matching phase and viscosity.[25] After introduction of the core and sheath flows into the device, hydrodynamic focusing laterally focuses the core fluid into a thin vertical stripe which spans the height of the channel (Figure 1). The flow-rate ratio between sheath and

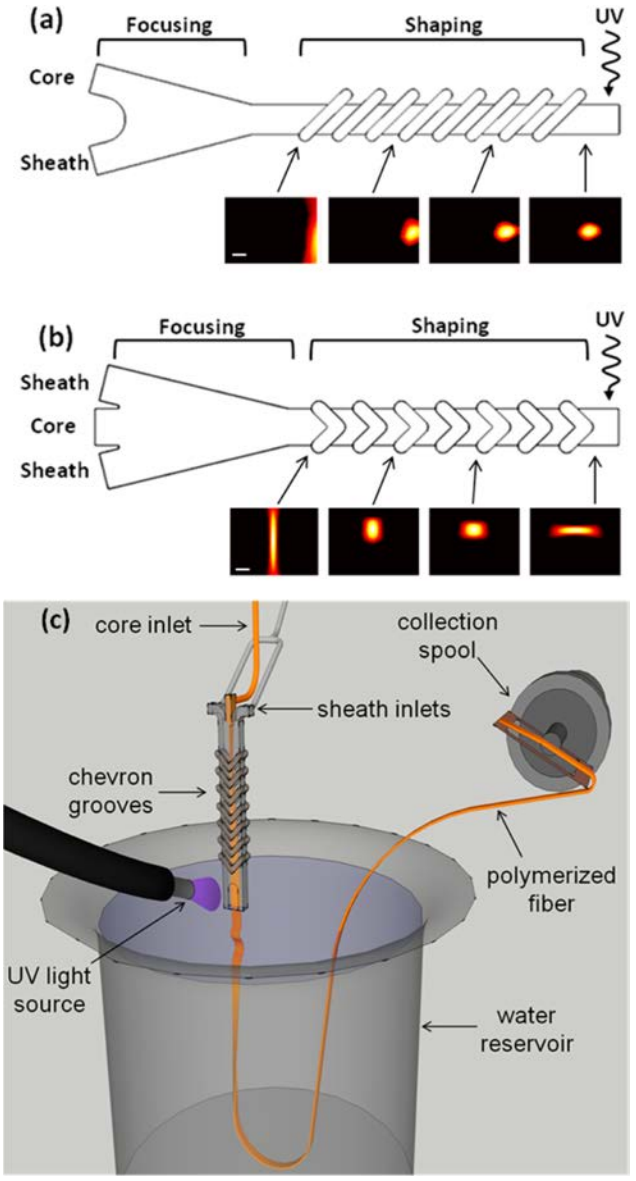

Figure 1. Channel schematics of devices and corresponding COMSOL simulations of fluid flows for fabrication of fibers with (a) round cross sections using eight diagonal grooves for shaping and (b) ribbon-shaped cross sections using seven chevron-shaped grooves. Channel schematics are viewed from the top and show the design of the channel inlets and the grooves used in each shaping region. Note that in part a the grooves are recessed into the floor and ceiling, while in part b the chevrons are recessed into the ceiling but project out of the floor. The COMSOL simulations are concentration plots showing the shape of the core beginning after the focusing region and showing the shape evolution as the prepolymer passes through the shaping region (scale bars represent 150 μm). Videos of the shaping simulations are available as web enhanced objects in quicktime format in the Supporting Information. (c) Diagram of the experimental setup for microfluidic fiber fabrication.

core determines the width of this stripe and the final cross-sectional area of the fiber after cross-linking. Downstream from the initial focusing region, a series of recessed grooves are patterned into the floor and ceiling of the channel. These grooves generate advection perpendicular to the channel axis such that the sheath fluid wraps around the core, focusing the core vertically and isolating the core fluid from the channel

dx.doi.org/10.1021/am3022834 | ACS Appl. Mater. Interfaces 2013, 5, 114−119

walls. The grooves are computationally designed in order to manipulate the core fluid into a desired cross-sectional shape.[26] Downstream from the shaping region, the core fluid is irradiated using high power UV light, cross-linking the thiol click material and locking in the cross-sectional shape. The device is vertically suspended with the channel exit submerged in a water bath. As the polymerized fiber exits the channel directly into a water bath, the sheath fluid is washed away and the fibers are collected for characterization by winding them onto a motorized spindle (Figure 1c).

In previous reports, a similar system produced acrylate fibers and liquid crystal-composite fibers,[27−29] in order to demonstrate the ability to shape the fibers (e.g., round, ribbon-shaped cross sections) using various designs of the channel grooves.[28,29] In the current work, two different devices generated fibers with round (Figure 1a) and ribbon-shaped (Figure 1b) cross sections. The device for producing round fibers had two inlets, one each for the core and sheath fluids. In this case, hydrodynamic focusing initially generated a vertical stripe that spanned the channel from floor to ceiling and that was positioned adjacent to the side wall on the core inlet side. Downstream from the focusing region, eight diagonal grooves were recessed into the channel walls. The grooves inclined 45° relative to the channel axis such that the sheath fluid flowed down the grooves at an angle to the channel and displaced the core fluid from the top, bottom, and side walls of the channel. After shaping, the core was essentially round, although there was a small, teardrop-shaped "tail" where the core fluid was last in contact with the channel side-wall (Figure 2a).

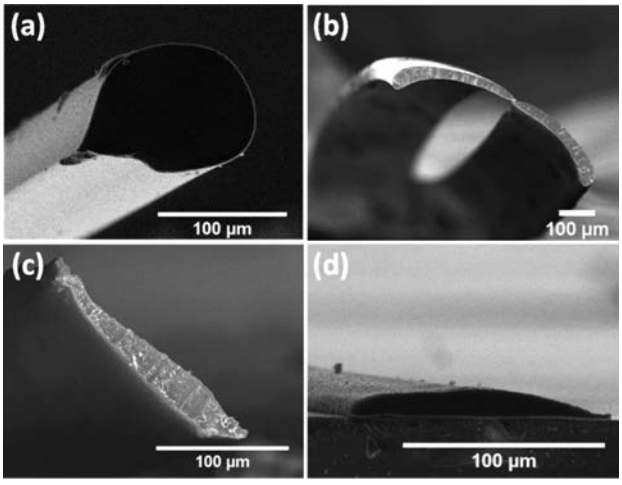

Figure 2. SEM cross-section images of thiol click fibers. (a) Round thiol−ene fiber (average diameter of 110 μm) fabricated using a sheath−core flow-rate ratio of 25:1. (b−d) Ribbon-shaped fibers generated at flow-rate ratios of 25:1, 50:1, and 100:1, respectively, with dimensions of (width × height) (b) 330 μm × 30 μm, (c) 190 μm × 20 μm, and (d) 125 μm × 10 μm. Images b and c are thiol−yne, and image d is thiol−ene.

Ribbon-shaped fibers were produced using a system with two sheath inlets and a central core inlet such that hydrodynamic focusing produced a vertical stripe situated in the center of the channel (Figure 1b). Downstream from the focusing region, the channel was patterned with seven chevron-shaped grooves in the top and bottom channel walls. Each chevron generated a rotational flow in each quadrant of the channel cross-section, such that the sheath fluid was pushed toward the top and bottom of the channel, displacing the core fluid away from these surfaces and eventually producing a ribbon-shaped core flow (Figure 1b).

An important aspect to the production of smooth, continuous fibers with the proper cross-sectional shape using our method is to employ core and sheath fluids whose viscosities are well-matched. When this is not the case, we have observed that viscous buckling of the core can occur and result in wavy, "knotted" fibers. To reduce the occurrence of viscous buckling while ensuring the proper fiber shape, we matched the viscosities of the core solutions with polyethylene glycol (PEG). We chose polyethylene glycol (PEG) as the sheathing solution because it has low toxicity, is miscible with all the reagents and solvents used, and has a viscosity that is a function of the molecular weight of the polymer.

Upon exposure to UV after the core fluid was focused and shaped, the step growth polymerization of the thiol click core solution caused a polymer fiber to form. A primary constraint on the system was that the polymerization must be rapid, as the exposure time at currently used flow rates was only on the order of 1 s. The UV light source was situated perpendicularly ∼1.5 cm from the vertical channel. The UV exposure region to the channel exit had to be long enough so that the polymerization of the fiber was virtually complete but not so long that the polymerized fiber could clog the end of the microchannel; clearly flow velocity and fiber size also played a part in determining the appropriate length of the channel. In the experiments reported here, the distance from the UV exposure region to the microchannel exit was ∼1 cm. Fibers were continually produced and collected until the prepolymer and sheath reservoirs were expended.

Fiber Size and Shape. As opposed to formation of thiol click fibers by electrospinning, in which the fiber size was largely dictated by the balance between the solution viscosity and the electric potential, the size of fibers produced by hydrodynamic focusing was easily adjusted by tuning the flow-rate ratio between sheath and core fluids. The SEMs demonstrated good agreement between the experimental results and the COMSOL simulated fiber shapes shown in Figure 1 and in the Supporting Information. Figure 2 shows typical examples of scanning electron micrographs (SEMs) of round and ribbon-shaped thiol click fibers.

The fiber cross-section remained consistent for each fiber size and shape for both the thiol−yne and thiol−ene materials. Depending on the flow-rate ratio (sheath:core), where both the sheath and core values are given in units of μL/min., the diameter of round fibers fabricated in these experiments ranged from 50 μm (100:1) to 110 μm (25:1). The cross-sectional dimensions for ribbon-shaped fibers produced in these experiments ranged from 125 μm × 10 μm (100:1) to 330 μm × 30 μm (25:1). The variability of the cross-sectional area measured over several centimeters along the length of a fiber was typically <1.0%. Figure 2a shows a round fiber with approximately the same cross-sectional area as the ribbon fibers in Figure 2b. Parts b, c, and d of Figure 2 show ribbon fibers all made in the same device but at different flow-rate ratios. Qualitatively, both the thiol−ene (Figure 2a,d) and thiol−yne (Figure 2b,c) fibers had smooth surfaces in SEM images and appeared transparent when viewed under an optical microscope.

A potential advantage of noncircular cross-section shapes is the increase in surface area-to-volume ratio compared to round fibers. The measured surface area-to-volume ratio for ribbon-

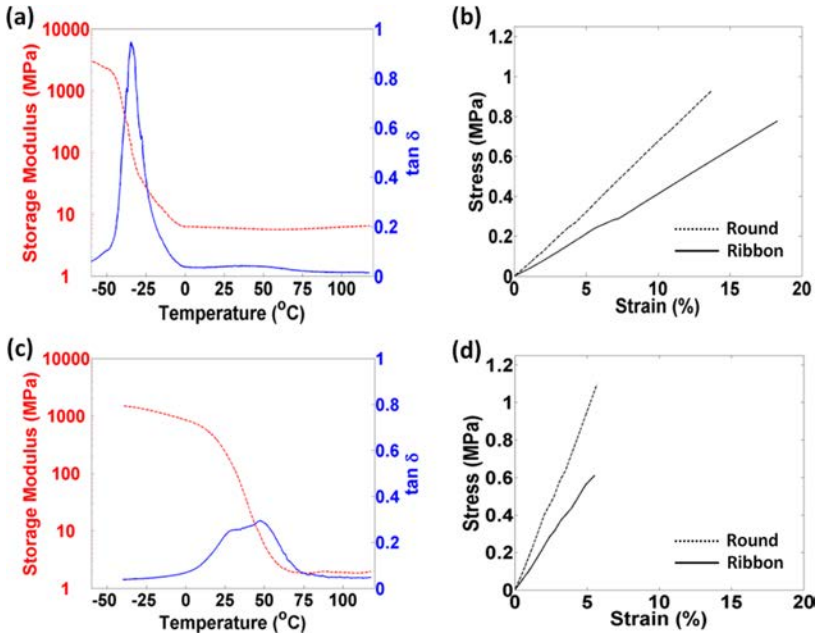

Figure 3. Dynamic mechanical analysis of thiol−ene (top row) and thiol−yne (bottom row) click fibers. (a) Storage modulus and tan δ of ribbon-shaped thiol−ene fibers. (b) Stress vs strain curves for round and ribbon-shaped thiol−ene fibers. (c) Storage modulus and tan δ of ribbon-shaped thiol−yne fibers. (d) Stress vs strain curves for round and ribbon-shaped thiol−yne fibers. All stress−strain curves depicted were taken at 80 °C.

shaped fibers (0.075) was twice that of the ratio for round fibers (0.038) at a sheath:core flow-rate ratio of 25:1.

Fiber Mechanical Properties. Dynamic mechanical analysis (DMA) was used to determine the Young's modulus and glass transition temperature (T_g) of the fibers, as shown in Figure 3. The Young's moduli values were determined at both 30 °C (near typical ambient temperatures) and 80 °C (above the T_g for both thiol−ene and thiol−yne fibers). The results indicated that thiol−yne fibers have greater stiffness as well as a greater T_g than their thiol−ene counterparts (Table 1). In general, these results confirmed that the mechanical properties of the hydrodynamically shaped fibers were comparable to values previously reported for films made from similar materials with significantly longer exposure times.[23]

Table 1. Mechanical Properties[a]

	avg Young's modulus (MPa)				
fiber type	30 °C	80 °C	T_g (°C)	ρ (M)	tan δ fwhm (°C)
round thiol−yne	15 ± 2	21 ± 2	47	2.2	46
ribbon thiol−yne	14.5 ± 0.4	12.6 ± 0.9			
round thiol−ene	5.3 ± 0.8	6.8 ± 0.1	−35	6.4	13
ribbon thiol−ene	2.3 ± 0.6	4.7 ± 0.1			

[a]Average Young's moduli, glass transition temperatures (T_g), cross-link densities (ρ at 65°C), and the tan δ full width at half maximum (fwhm) of 8−10 round and ribbon-shaped thiol click fibers as determined by dynamic mechanical analysis (DMA).

Further analysis using DMA also indicated that the typical breaking strains of thiol−yne fibers were lower than those for thiol−ene fibers, as seen in Figure 3c,d. The data also indicated that, independent of the thiol material, round fibers tended to be slightly stiffer (larger Young's modulus) than ribbon-shaped fibers. While we are aware of comparisons of round and ribbon-shaped carbon fibers, our literature searches produced no other studies comparing stiffness vs shape in polymer fibers, and we have no good explanation for this observation: it warrants further investigation.

Fiber Surface Functionality Assay. One of the most desirable features of thiol click materials is the ease with which surface functionality can be incorporated by merely adjusting the thiol to alkyne (or alkene) stoichiometric ratio in the prepolymer solution to have excess thiols. As there is no constraint on solution viscosity using the hydrodynamic fiber fabrication method, the stoichiometric ratio of the components used to generate fibers could be varied.[23] A prepolymer solution with a stoichiometric mix designed to produce free thiols after polymerization was tested for the availability of surface thiols for subsequent modification using a simple dipping experiment (Scheme 1). Fibers with putative excess thiols were immersed in a maleimide-polyethylene glycol$_2$-biotin solution. Following a wash, the fibers were then incubated in a solution of streptavidin-phycoerythrin. If free thiols were present on the surface and available for reaction, the maleimide-polyethylene glycol$_2$-biotin would bind to them, providing a biotin to capture the fluorescent streptavidin-phycoerythrin label. Two controls were included in this experiment: First, a fiber that was not modified following polymerization was imaged to measure any inherent auto-fluorescence in the thiol−yne material. Second, a thiol−yne fiber was introduced to streptavidin-phycoerythrin but not the maleimide-polyethylene glycol$_2$-biotin; fluorescence would indicate nonspecific binding of the streptavidin-phycoerythrin tag to the surface of the fibers.

The results showed that the fiber incubated with maleimide-polyethylene glycol$_2$-biotin followed by streptavidin-phycoerythrin had high levels of fluorescence, whereas the controls did not (Figure 4). The difference was at least a factor of 10. A cross section of the fiber, which was imaged end-on by

dx.doi.org/10.1021/am3022834 | ACS Appl. Mater. Interfaces 2013, 5, 114−119

Scheme 1. Binding of Maleimide-PEG$_2$-Biotin to Excess Thiols on the Surface of a Thiol−yne Fiber, Followed by the Attachment of Fluorescent Streptavidin-Phycoerythrin to the Biotin Tag

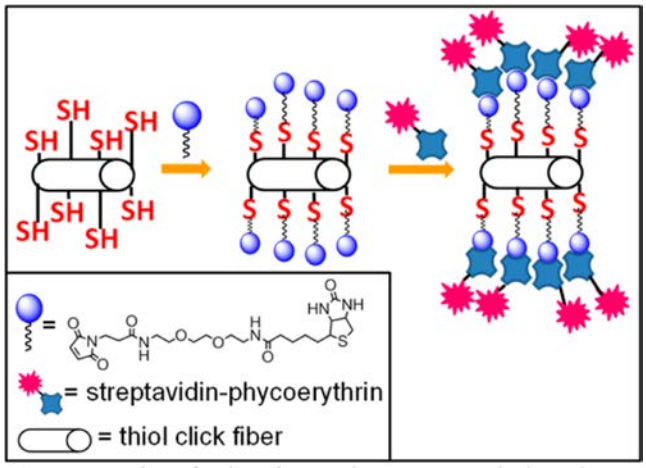

fluorescence microscope, showed that the fluorescence was localized at the surface rather than throughout the interior of the fiber (Figure 4e). The incubation periods for the test and control fibers in streptavidin-phycoerythrin were varied from an hour up to 18 h in separate assay runs, and the results were consistent regardless of the incubation period. These data specifically indicated the presence of free thiols on the fiber surface available for subsequent modification and the capability of the modified fibers to be used for target binding.

CONCLUSION

We demonstrated the ability to produce thiol click fibers with predetermined size and shape in a facile manner using hydrodynamic focusing. The method can be used with prepolymers of varying viscosity and composition. Specifically, we reported the first instance of thiol−ene fibers formed via microfluidic fabrication and the first description of thiol−yne fibers produced via any fabrication process. In addition, the surface of fibers fabricated with free surface thiols was subsequently functionalized with a covalently attached ligand. These functionalized fibers demonstrated specific capture of a fluorescent protein. The ability not only to make fibers "to design" but also to modify them with a variety of functional ligands should lead to new smart materials for sensing, filtration, and textile applications.

EXPERIMENTAL SECTION

Chemicals and Materials. Pentaerythritol tetrakis (3-mercaptopropionate) (PETMP); 1,7-octadiyne (ODY); 1,4-butanediol divinyl ether (BDDVE); 2,2-dimethoxy-2-phenylacetophenone (DMPA); 1,6-hexanedithiol (HxDT); (1,3,5-triallyl-1,3,5-triazine-2,4,6 (1*H*,3*H*,5*H*)-trione (TATATO); 1,6-heptadiyne (HpDY); and polyethylene glycol (PEG) MW 400 were all purchased from Sigma Aldrich. Maleimide-polyethylene glycol$_2$-biotin was purchased from Thermo Scientific. Streptavidin-phycoerythrin was purchased from Life Technologies.

Prepolymer Solution Preparation. Thiol−yne fibers were made by combining 1 equiv of ODY (0.0094 mol) with 1 equiv of PETMP (0.0094 mol). Thiol−ene fibers were made by combining 2 equiv of BDDVE (0.0094 mol) with 1 equiv of PETMP (0.0047 mol). For fiber polymerization, 2 mol % DMPA photoinitiator was added to the intended thiol−yne or thiol−ene solution. Solutions were immediately transferred to a syringe for introduction into the microfluidic channel. Each solution was made and handled under limited light conditions to prevent premature polymerization.

Fiber Fabrication. Fibers were shaped and polymerized using diagonal (round fibers) or chevron (ribbon-shaped fibers) grooves in a microfluidic channel setup as previously described.[25,28,29] The channels were 750 μm high and 1000 μm wide, while the grooves were 250 μm deep and 250 μm across. Polymerization utilized UV irradiation at 365 nm and ∼200 mW/cm^2. The UV light source was perpendicularly oriented ∼1.5 cm from the vertical channel. The distance from the UV exposure region to the microchannel exit was ∼1 cm. All fibers reported in Table 1, as well as fibers used in the fluorescence tagging assay, were fabricated with sheath:core flow-rate ratios of 25:1. The disappearance of thiol, alkene, and alkyne bands was monitored by FT-IR (Bruker Tensor 27/Opus Data Collection, Billerica, MA).

Scanning Electron Microscope Imaging. For cross-section shape imaging purposes, polymerized fibers were cut using a razor. Fibers were coated with ∼50 nm of gold/palladium via sputter coating (Cressington Auto 108 Sputter Coater, Ted Pella Inc., Redding, CA). Following sputter coating, fiber images were obtained using a LEO Supra 55 scanning electron microscope (Carl Zeiss SMT Inc., Peabody, MA).

Tensile Analysis. Stress versus strain was measured by alignment of 8 to 10, 1.8 cm long fibers onto a small custom-built Dynamic Mechanical Analysis (DMA) alignment device (see the Supporting Information, Figure S3). The uniformly aligned fibers were clamped into a DMA instrument (Q800 series TA Instruments, New Castle, DE). Tensile modulus was determined at two temperatures (30 and 80 °C) with the force on the fibers being ramped from 0.004 N to an upper limit of 3.300 N at a rate of 0.005 N/min. A slope was then calculated from a plot of the stress versus strain curve at low strain. Determination of the glass transition temperature (T_g) and tan δ of the

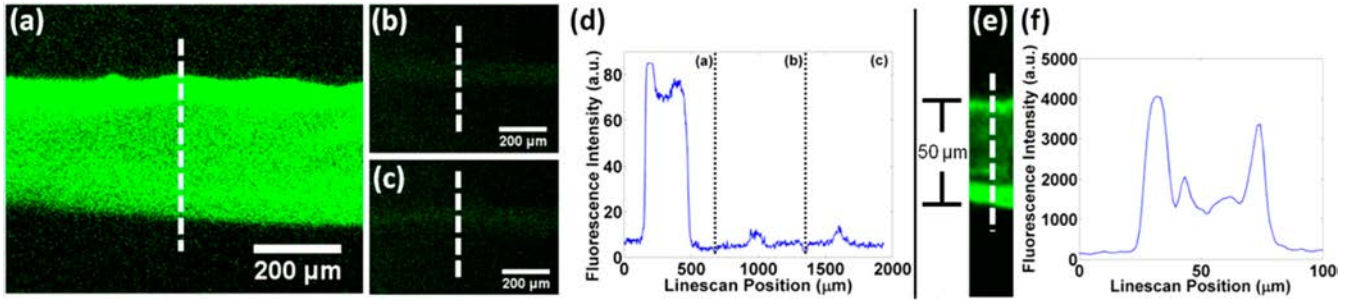

Figure 4. Fluorescence experiment on 2:1 stoichiometrically imbalanced thiol−yne fibers demonstrating a fluorescent label specifically bound via a maleimide linker to free thiols on the fiber surface. Line scans of the fluorescence intensity across the experimental fiber (a) and control fibers (b and c) are displayed in part d and demonstrate significant binding to the experimental fiber only. The cross-sectional fluorescence image (e) and intensity linescan (f) of a labeled fiber demonstrate that the fluorescence is largely confined to the surface. Each line scan is the average fluorescence intensity of roughly 10 line scans taken in the vicinity of the vertical white dotted lines overlaid on each fluorescence image.

dx.doi.org/10.1021/am3022834 | ACS Appl. Mater. Interfaces 2013, 5, 114−119

fibers was also done using the DMA instrument. T_g and tan δ values were determined by ramping the temperature from −60 to 120 °C at a rate of 3 °C/min. The cross-link density was calculated based on the theory of rubber elasticity and assumed the materials were incompressible.[23] The tan δ fwhm values were determined as the full width of the tan δ at half of its maximum value.

Surface Fluorescence Experiment. Thiol−yne fibers were prepared as described above, with the exception that the stoichiometry was adjusted such that the ratio of thiol-to-alkyne was 2:1 (i.e., 8 thiols to 2 alkynes). The fibers were washed with phosphate buffered saline with 0.1% Tween (PBST) and then incubated in an 8 mM solution of maleimide-polyethylene glycol$_2$-biotin for 2 h. Following incubation in maleimide-PEG$_2$-biotin, the fibers were washed with PBST and then incubated in 0.010 mg/mL streptavidin-phycoerythrin for 18 h. The fibers were again washed with PBST. Fluorescence imaging of the fibers was performed at an excitation wavelength of 488 nm on a fluorescent microscope (Nikon TE2000-E).

■ ASSOCIATED CONTENT

Supporting Information

Structures and combinations for additional fibers, FT-IR plot of thiol−yne, description of COMSOL simulations, and DMA alignment apparatus information. This material is available free of charge via the Internet at http://pubs.acs.org.

■ AUTHOR INFORMATION

Corresponding Author

*E-mail: frances.ligler@nrl.navy.mil.

Author Contributions

‡These authors contributed equally.

Notes

The authors declare no competing financial interest.

■ ACKNOWLEDGMENTS

The authors wish to thank Chris R. Taitt, Christopher M. Spillmann, Peter B. Howell, and Peter Matic for helpful suggestions during the course of these experiments. We would also like to acknowledge a summer student, Colleen O'Neil, for work she did related to this project. Darryl A. Boyd and Adam R. Shields are National Research Council Postdoctoral Fellows. The work was supported by ONR/NRL Work Unit 9899. The views are those of the authors and do not represent the opinion or policy of the U.S. Navy or Department of Defense.

■ REFERENCES

(1) Posner, T. *Ber. Dtsch. Chem. Ges.* **1905**, *38*, 646−657.
(2) Kharasch, M. S.; Read, J.; Mayo, F. R. *Chem. Ind. (London)* **1938**, *57*, 752−754.
(3) Kohler, E. P.; Potter, H. *J. Am. Chem. Soc.* **1935**, *57*, 1316−1321.
(4) Hoyle, C. E.; Bowman, C. N. *Angew. Chem., Int. Ed.* **2010**, *49*, 1540−1573.
(5) Hoyle, C. E.; Lowe, A. B.; Bowman, C. N. *Chem. Soc. Rev.* **2010**, *39*, 1355−1387.
(6) Lowe, A. B.; Hoyle, C. E.; Bowman, C. N. *J. Mater. Chem.* **2010**, *20*, 4745−4750.
(7) Aimetti, A. A.; Machen, A. J.; Anseth, K. S. *Biomaterials* **2009**, *30*, 6048−6054.
(8) Lin, C.-C.; Raza, A.; Shih, H. *Biomaterials* **2011**, *32*, 9685−9695.
(9) Nimmo, C. M.; Shoichet, M. S. *Bioconjugate Chem.* **2011**, *22*, 2199−2209.
(10) Daniele, M. A.; North, S. H.; Naciri, J.; Howell, P. B.; Foulger, S. H.; Ligler, F. S.; Adams, A. A. *Adv. Funct. Mater.* **2012**, DOI: 10.1002/adfm.201202258.
(11) Killops, K. L.; Campos, L. M.; Hawker, C. J. *J. Am. Chem. Soc.* **2008**, *130*, 5062−5064.
(12) Montanez, M. I.; Campos, L. M.; Antoni, P.; Hed, Y.; Walter, M. V.; Krull, B. T.; Khan, A.; Hult, A.; Hawker, C. J.; Malkoch, M. *Macromolecules* **2010**, *43*, 6004−6013.
(13) Service, R. F. *Science* **2008**, *320*, 868−869.
(14) Lu, H.; Carioscia, J. A.; Stansbury, J. W.; Bowman, C. N. *Dent. Mater.* **2005**, *21*, 1129−1136.
(15) Carioscia, J. A.; Lu, H.; Stanbury, J. W.; Bowman, C. N. *Dent. Mater.* **2005**, *21*, 1137−1143.
(16) Davis, A. R.; Maegerlein, J. A.; Carter, K. R. *J. Am. Chem. Soc.* **2011**, *133*, 20546−20551.
(17) Kwisnek, L.; Kaushik, M.; Hoyle, C. E.; Nazarenko, S. *Macromolecules* **2010**, *43*, 3859−3867.
(18) Shanmuganathan, K.; Sankhagowit, R. K.; Iyer, P.; Ellison, C. J. *Chem. Mater.* **2011**, *23*, 4726−4732.
(19) Chan, J. W.; Hoyle, C. E.; Lowe, A. B.; Bowman, M. *Macromolecules* **2010**, *43*, 6381−6388.
(20) Lee, T. Y.; Cramer, N. B.; Hoyle, C. E.; Stansbury, J. W.; Bowman, C. N. *J. Polym. Sci. Polym. Chem.* **2009**, *47*, 2509−2517.
(21) Cramer, N. B.; Scott, J. P.; Bowman, C. N. *Macromolecules* **2002**, *35*, 5361−5365.
(22) Hensarling, R. M.; Doughty, V. A.; Chan, J. W.; Patton, D. L. *J. Am. Chem. Soc.* **2009**, *131*, 14673−14675.
(23) Fairbanks, B. D.; Scott, T. F.; Kloxin, C. J.; Anseth, K. S.; Bowman, C. N. *Macromolecules* **2009**, *42*, 211−217.
(24) Fairbanks, B. D.; Sims, E. A.; Anseth, K. S.; Bowman, C. N. *Macromolecules* **2010**, *43*, 4113−4119.
(25) Howell, P. B.; Ligler, F. S.; Shields, A. R. *Sheath Flow Device and Method*. U.S. Patent Application 20110193259, August 11, 2011.
(26) Mott, D. R.; Howell, J. P. B.; Golden, J. P.; Kaplan, C. R.; Ligler, F. S.; Oran, E. S. *Lab Chip* **2006**, *6*, 540−549.
(27) Shields, A. R.; Spillmann, C. M.; Naciri, J.; Howell, P. B.; Thangawng, A. L.; Ligler, F. S. *Soft Matter* **2012**, *8*, 2656−2660.
(28) Thangawng, A. L.; Howell, P. B.; Richards, J. J.; Erickson, J. S.; Ligler, F. S. *Lab Chip* **2009**, *9*, 3126−3130.
(29) Thangawng, A. L.; Howell, P. B.; Spillmann, C. M.; Naciri, J.; Ligler, F. S. *Lab Chip* **2011**, *11*, 1157−1160.